Chapter 17
Biomaterials Made from Coiled-Coil Peptides

Vincent Conticello, Spencer Hughes, and Charles Modlin

Contents

Abstract The development of biomaterials designed for specific applications is an important objective in personalized medicine. While the breadth and prominence of biomaterials have increased exponentially over the past decades, critical challenges remain to be addressed, particularly in the development of biomaterials that exhibit highly specific functions. These functional properties are often encoded within the molecular structure of the component molecules. Proteins, as a consequence of their structural specificity, represent useful substrates for the construction of functional biomaterials through rational design. This chapter provides an in-depth survey of biomaterials constructed from coiled-coils, one of the best-understood protein structural motifs. We discuss the utility of this structurally diverse and functionally tunable class of proteins for the creation of novel biomaterials. This discussion illustrates the progress that has been made in the development of coiled-coil biomaterials by showcasing studies that bridge the gap between the academic science and potential technological impact.

Keywords Coiled-coils • Biomaterials • Hydrogels • Nanotubes • Nanomedicine

V. Conticello (✉) • S. Hughes • C. Modlin
Emory University Chemistry Department, 1515 Dickey Drive, Atlanta 30322, Georgia
e-mail: vcontic@emory.edu

D.A.D. Parry, J.M. Squire (eds.), *Fibrous Proteins: Structures and Mechanisms*,
Subcellular Biochemistry 82, DOI 10.1007/978-3-319-49674-0_17

Abbreviations

PHPMA	poly (N-(2-hydroxypropyl))methylacrylamide
MTX	methotrexate
RHCC	Right-handed coiled-coil
EPR	Enhanced permeability and retention
NHL	Non-Hodgkin's Lymphoma
RGD	Arginine-Glycine-Aspartate
LZ	leucine zipper
HPMA	N(2-hydroxypropyl)methylacrylamide
DAMA	N',N'-(dicarboxymethylaminopropyl)methacrylamide
MTS	3-(4,5-dimethylthiazol-2-yl)-5-(3-carboxymethoxyphenyl)-2-(4-sulphophenyl)-2H-tetrazolium
COMP	cartilage oligomeric matrix protein
PEGDA	polyethylene glycol diacrylate
hSAFs	hydrogelating self-assembling fibres
SAFs	self-assembling fibres
AUC	analytical ultra centrifugation
SARS	Severe Acute Respiratory Syndrome
SMCC	The N-hydroxysuccinimide ester of 4-(N-maleimidomethyl) cyclohexanecarboxylic acid

17.1 Introduction: The Emerging Role of Biomaterials

Biomaterials derived from designed peptide and protein sequences have become the focus of significant scientific research effort over the last two decades. Rapid developments in genome sequencing, bioinformatic analysis, atomic resolution structural determination, and computational protein design, in combination with extant synthetic and analytical methods, present an unprecedented opportunity to create peptide- and protein-based biomaterials of defined structure and controllable function. Progress toward the goal of creating tailorable biomaterials for applications in nanotechnology and human health has been impressive, although the practical promise has yet to be realized on a substantial scale. One strategy has involved the identification of stable structural motifs that can serve as flexible scaffolds for the introduction of function. This approach requires the identification of protein folds that can accommodate substantial sequence modification without compromising structure or function. Ideally, these protein motifs would be highly designable and amenable to computational structural prediction. The α-helical coiled-coil motif is the most studied protein fold and fulfills many of the criteria that one would envision as a scaffold for biomaterials design.

In recent years, the well-known coiled-coil motif has been widely employed in the generation of novel biomaterials. The canonical coiled-coil, comprised of two

(or more) right-handed α-helices, is a left-handed super-helix wherein the constituent α-helices have a crossing angle (angle between two helices of a coiled-coil (Lupas 1996) of roughly 20° (Lupas and Gruber 2005)). However, minute mutations to the primary sequence can produce profound changes that can cause the coiled-coil to deviate from the classical coiled-coil definition referenced above (Zimenkov et al. 2006; Wood et al. 2014). Such deviations, such as stutters and stammers, often alter the resultant biophysical properties of the coiled-coil (Gruber and Lupas 2003). Coiled-coils present multiple advantages as biomaterials scaffolds, including:

1. Well-understood design rules (Lupas and Gruber 2005)
2. Accessibility of a variety of oligomeric states (Harbury et al. 1993)
3. Dynamic responsiveness to environmental factors (Zimenkov et al. 2006; Dublin and Conticello 2008; Banwell et al. 2009)
4. Versatility in sequence and structure
5. Biocompatibility

As discussed in previous chapters, coiled-coils can be designed *de novo* using a handful of simple rules that can be implemented computationally to select for oligomerization state with a great degree of reliability (Thompson et al. 2014; Huang et al. 2005; Wood et al. 2014).

Hydrophobic residues usually occupy a majority of the core *a* and *d* positions of the heptad repeats. Charge complementarity can be employed at proximal positions to control helix alignment or promote the formation of heteromeric assemblies. Sequence control of the residues that occupy the (*a, d, e, g*) positions, which define the extended helix-helix interface, can be employed to control the oligomerization state in the range from 2 to 7 helices. In contrast, design rules (Grigoryan and DeGrado 2011) to specify the formation of specific super-secondary or tertiary structures are not as readily apparent for β-strand-based biomaterials, or, at this juncture, more complex structural motifs. By explicit design, coiled-coils have been developed with environmental "switches"; in which a pH drop might cause dissociation of a coiled-coil into its constituent helices, or a metal ion may induce a registry shift (Fig. 17.1), leading to an exclusive population of one oligomeric structure (Anzini et al. 2013).

As evidenced by their ubiquity in the proteomes of sequenced organisms, coiled-coil proteins comprise varied sequences, adopt a variety of native structures, and display a range of functions (Testa et al. 2009). The scope of coiled-coil sequences and structures has been further expanded through the carefully applied use of rational design. Non-canonical amino acids can be incorporated at specified sites in the sequences using either solid-phase peptide synthesis methods or supplementation of growth media used in *in vitro* or *in vivo* protein expression. The introduction of non-native chemical functionality can further expand the material properties of this flexible scaffold. Indeed, coiled-coils are a versatile and robust scaffold for generating a diverse range of functional biomaterials that can be tailored for specific applications through modification of the sequence at structurally permissive sites.

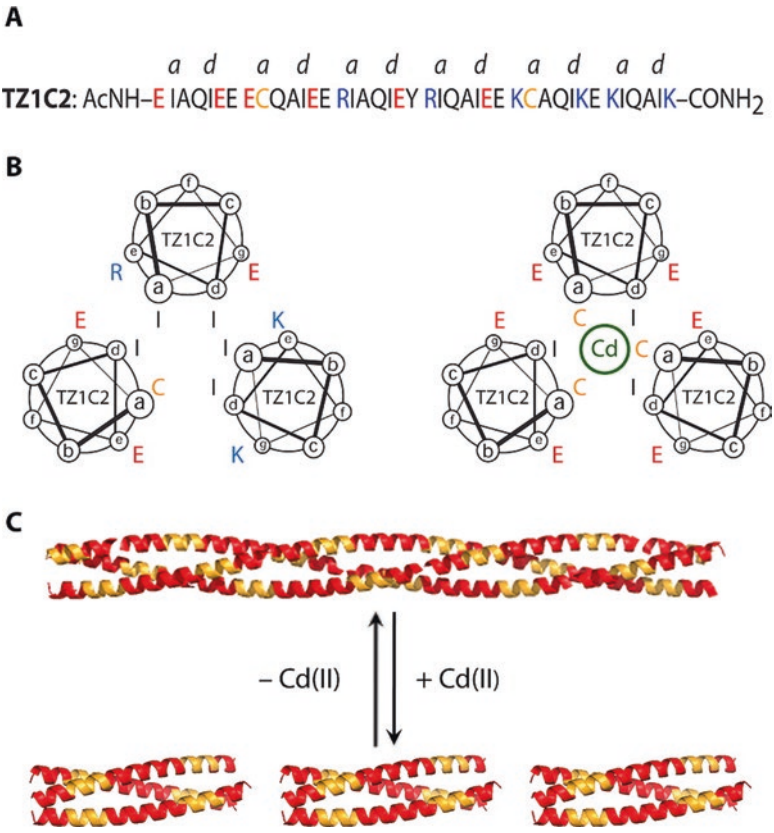

Fig. 17.1 Design of a metal-ion induced registry shift into a trimeric coiled-coil structure. Briefly, Cd^{2+} ions coordinate with cysteine sidechains in the coiled-coil's hydrophobic core, locking them into a trimeric state, rather than the off-register fibrillar structure seen in non-metallated samples. (**a**) Single-letter amino acid sequence of the TZ1C2 peptide, with the *a* and *d* positions labelled to highlight the hydrophobic core of the coiled-coil structure. (**b**) Helical-wheel representations of the out-of-register (*left*), metal-free peptide, and the in-register (*right*), metal-coordinated peptide. (**c**) Fibre representation of the metal-ion oligomerization switch (Reprinted with permission from Anzini et al. (2013) Copyright 2013 *J Am Chem Soc*)

17.2 Coiled-Coil Therapeutics

A major problem facing modern medicine is the dearth of strategies for treating diseases that present differently in each patient, e.g. cancer. The need for easily customizable treatments has led to the development of a broad field known as nano-theranostics (a portmanteau derived from therapeutics and diagnostics), which seeks to use nano-scale materials to image and/or treat diseases. A dominant strategy in nano-theranostics is to specifically target diseased cells for the delivery of small doses of extremely cytotoxic low molecular weight drugs. A clear challenge in this field is thus developing site-specific drug delivery to reduce side effects from

apoptosis of healthy cells. Coiled-coil motifs have recently been explored as potential nano-theranostic agents, due to their lack of immunogenicity, exquisite sensitivity to biologically relevant environmental changes (such as pH), and well-known engineering rules. This inherent designability makes coiled-coils an attractive scaffold from which to develop materials for nano-scale treatments.

Coiled-coil-based therapeutics can be broken up into two main categories: coiled-coil drug carriers, and drug-free coiled-coil systems. The first of these categories is more familiar to those studying nano-medicine. Essentially, a low molecular weight drug is encapsulated by a self-assembling coiled-coil, which dissociates upon some environmental change (typically pH, which can vary in a diseased state) (Yu 2002). The low molecular weight drug is generally highly cytotoxic and, as such, the design focus for this approach is towards target specificity (Pola et al. 2013). These systems also offer the potential for multi-valent drug binding, which improves the loading efficiency by minimizing the entropic penalty for binding. Assuming one chain in a heterodimeric coiled-coil system contains a single binding site, its sequence may be doubled to introduce a second binding site (Assal et al. 2015). Recently, Klok and co-workers investigated a heterodimeric coiled-coil carrier comprising two peptides (K_3 and E_3), which self-assemble at pH 7.0, but dissociate at pH 5.0 (endosomal pH), thereby releasing their cargo (Apostolovic et al. 2010, 2011). These peptides were bound to a poly (N-(2-hydroxypropyl)-methacrylamide (PHPMA) polymer backbone and designed to carry an anti-cancer drug, methotrexate (MTX) in one case, and a fluorescent dye in another. By combining these two technologies, it follows that one could monitor cellular uptake of the drug carrier while simultaneously treating the patient. Though uptake of the drug into the endosomes was shown, the distribution of the drug throughout the organelles has not yet been obtained.

In a more direct therapeutic solution, Thanasupawat et al., recently reported a coiled-coil-based system with improved selectivity that targets gliomas (malignant tumours that bud from glial cells in either the brain or the spine) (Thanasupawat et al. 2015). Briefly, they developed a right-handed coiled-coil (RHCC) comprising four identical alpha helices. Each alpha helix presents a methionine residue on the solvent-exposed surface of the tube, through which it coordinates a Platinum (IV) ion derived from tetrachloroplatinate (Fig. 17.2). The complexed Pt(IV) displayed a stronger selectivity for the target tumour and less cytotoxicity than the more labile cis-platin derivative of the RHCC. The RHCC essentially serves as a carrier for four equivalents of the Pt(IV) complex, which acts as a pro-drug that is activated via conversion to the therapeutic Pt(II) state in the reductive environment of the tumour cell. This phenomenon affords higher efficacy and fewer side effects, resulting in minimization of treatment cost and duration.

The second approach involves grafting of coiled-coil peptides to a synthetic polymer backbone; upon self-assembly, the polymer-peptide complex induces a physiological change in the cell that triggers apoptosis (Pechar et al. 2011). Although this approach has only recently emerged, it presents a strong advantage over drug-based therapies; namely, none of the components acting alone can induce apoptosis. Assuming specific bio-recognition of the constituent peptides, apoptosis will only

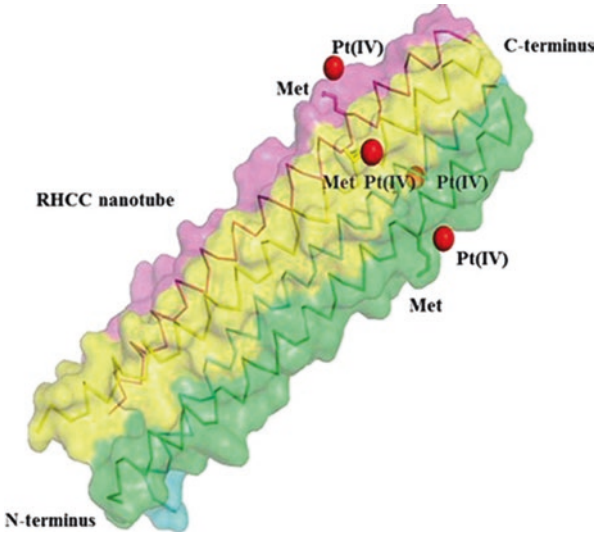

Fig. 17.2 Complex comprising four alpha-helices in a right-handed coiled coil conformation with four coordinated Pt(IV) ions (*red spheres*) (Reprinted with permission from Thanasupawat et al. (2015) Copyright 2015 *Nanomedicine*)

occur at the diseased cell. This represents a new paradigm in nanomedicine, and was pioneered by Kopeček and co-workers (Wu et al. 2012; Chu and Kopeček 2015). These researchers developed the idea of attaching high molecular weight polymers to small coiled-coil-forming peptides. The biocompatible polymer is linked to one peptide to increase endocytosis by cancer cells, via the enhanced permeability and retention (EPR) effect. This effect states that due to the increased vasculature and poor draining of tumour cells, high molecular weight polymers are more likely to be endocytosed than smaller species, and are also less likely to be drained through the lymphocytes. A second peptide, complementary to the first, is conjugated to a receptor recognition motif, which directs the peptide to a cell type of interest. The Kopeček group explored the use of these materials for the treatment of Non-Hodgkin's Lymphoma (NHL). In NHL, a specific surface receptor (CD20) is present on >95 % of tumourous cells. CD20 is also present on healthy B cells, but not on stem cells. It has been shown that the temporary B cell depletion is not deleterious. The recognition motif present on a specific antibody (Fab') is used as the targeting moiety in this model system. Fab' and its peptide partner bind to the CD20 receptors, and the peptide-polymer conjugates are effectively drawn towards the B cells. At this point, the peptides interact to form a heterodimeric coiled-coil, which induces cross-linking of the CD20 receptors. The cross-linking of CD20 receptors results in apoptosis, and effective remediation of the disease (Fig. 17.3).

17.3 Coiled-Coil Hydrogels

Hydrogels are formed from covalent or non-covalent cross-linking of individual polymer chains into a three-dimensional water-swollen network. Hydrogel materials offer a wealth of potential applications (Elisseeff 2008), in that the biological,

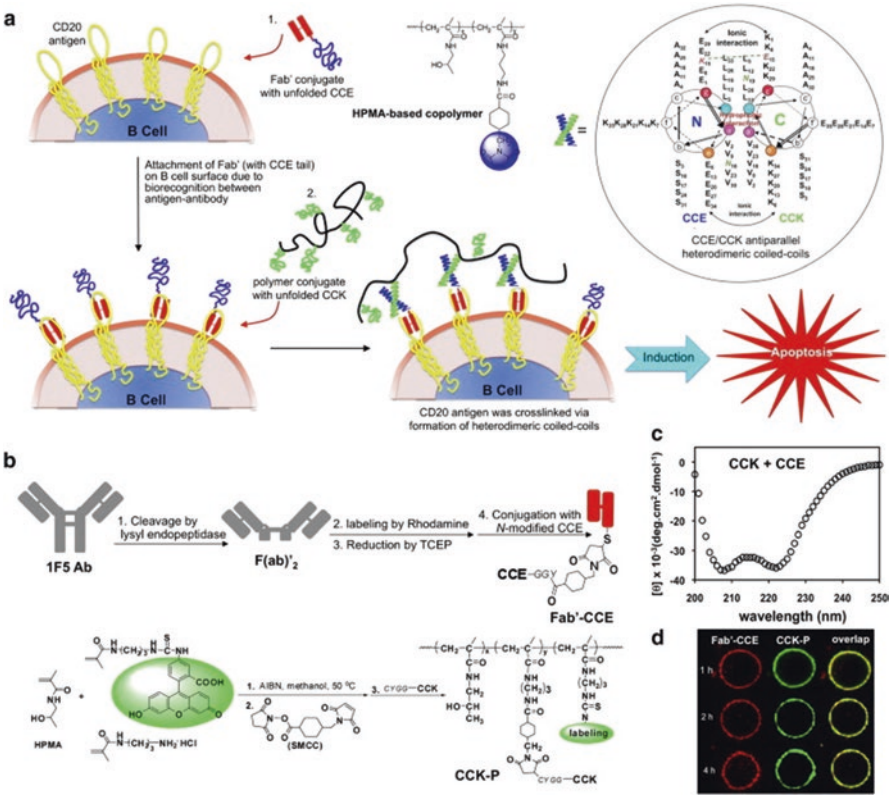

Fig. 17.3 Schematic representation of the drug-free coiled-coil-based therapeutics employed by the Kopeček group. The unfolded CCE peptide (*blue coil*) is chemically conjugated to the Fab' recognition domain (*red*), which directs it to the CD20 antigen (*yellow*). Unfolded CCK peptide (*green coil*) is directed to the cell surface via the EPR effect and conjugation to the HPMA copolymer backbone (*black coil*). Coiled-coil formation by the two peptides results in CD20 antigen crosslinking and subsequent apoptosis (Reprinted with permission from Wu et al. (2012) Copyright 2012 *J Control Release*)

chemical, and mechanical properties may be tailored for particular applications through modification of the structure of the polymer and cross-linker. They have innate capacity to absorb and retain large volumes of water relative to the mass of the hydrogel itself (Elisseeff 2008; Xu and Kopeček 2008; Yao et al. 2014). Moreover, hydrogels are often highly biocompatible due to their capacity for water absorption, physical elasticity, and relative softness (Kopeček 2007, Yao et al. 2014). The aforementioned qualities make hydrogels a convincing substitute for native extracellular matrix (Slaughter et al. 2009; Yao et al. 2014), as well as suitable candidates for cell culture applications (Frampton et al. 2011; Jung et al. 2011), biomedical uses such as wound treatment (Wong et al. 2011; Lin et al. 2011), and drug delivery (Garbern et al. 2011; Guziewicz et al. 2011). Unsurprisingly, hydrogels were the first biomaterials developed for medical uses in humans (Kopeček

2007; Kopeček and Yang 2012). As biomedical materials, coiled-coil-based hydrogels offer an alternative to the more commonly employed β-sheet hydrogels. One potential concern with the latter materials is that the β-sheet morphology is analogous to amyloid structures, such as those observed in prion and amyloid diseases. These toxic assemblies often develop via a misfolding of endogenous proteins and can be auto-catalytically propagated in the presence of a β-sheet template (Fletcher et al. 2011). Due to the risk of initiating protein misfolding disease states, implementation of β-sheet-based hydrogels must be carefully scrutinized for the manifestation of deleterious physiological effects (Fletcher et al. 2011). Biomaterials based on coiled-coil structures do not display similar behaviour, as self-assembly in most cases is restricted to the formation of closed oligomers. This section will cover the past decade of advances within coiled-coiled-based hydrogels.

Hydrogels based on coiled-coil self-association can offer several notable advantages (Kopeček 2007). The coiled-coil is an exceptionally well understood structural motif, when compared to other protein folding domains (*vide supra*) (Lupas and Gruber 2005). Due to the wealth of information regarding the coiled-coil's structure and properties (in comparison to other super-secondary and tertiary structures), the coiled-coil has the potential to serve as an ideal 'tuning knob' for hydrogel properties. Though the coiled-coil is certainly not the only factor that governs hydrogel properties, it represents the most facile mechanistic handle. Tuning coiled-coil properties can involve a procedure as simple as altering the sequence of amino acids within the constituent alpha helices, allowing the researcher to alter hydrogel properties with relative ease and efficiency. Coiled-coils offer versatility in terms of oligomeric state as well (Harbury et al. 1993). Moreover, due to the widespread prevalence of coiled-coils within native proteins, coiled-coil-based biorecognition domains are also pervasive throughout the natural world. Co-opting such domains may yield significant advantages in the engineering and design of hydrogels, as doing so may offer a conduit through which artificially engineered hydrogels may interact with natural systems with high specificity (Kopeček 2007).

For the purpose of this review two primary categories for *self-assembling* hydrogels exist: those that consist only of peptide/protein and those that are based on hybrid materials (Kopeček 2007). The latter incorporate non-peptidic moieties within the component molecules of the hydrogel. The most common protein hydrogels derived from coiled-coils are based on an ABA triblock copolymer architecture. Petka et al. developed the first ABA triblock polymer system for the fabrication of hydrogels (Petka et al. 1998). Subsequently, Xu and Kopeček further developed these materials. These *ABA* triblock copolymers comprise a sequence in which coiled-coil motifs occupy the endblock domains (*A*) while a hydrophilic random coil sequence (*B*) defines the midblock (Fig. 17.4). Self-association of alpha helical (*A*)-end-blocks initiates cross-linking of the polymers into a water-swollen network in which the hydrophilic (*B*) mid-block connects the coiled-coil domains (Kopeček 2007).

The self-assembly of these ABA block copolymers is driven by two interconnected forces: hydrophobic collapse of A ends and polar association of water with the B interior region. One advantage of hydrogel formation from these ABA block

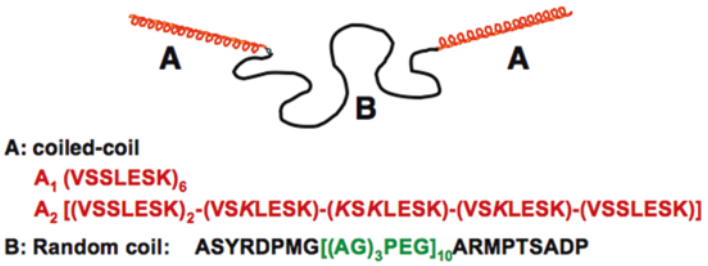

Fig. 17.4 Graphical representation of ABA triblock copolymer system pioneered by the Kopeček group, wherein *A* ends (shown in *red*) are alpha helices and the *B* middle (shown in *black*) is a random coil. The *A* helix ends associate with neighbouring *A* helices to form coiled-coils, generating a coiled-coil-based hydrogel. The sequences used by the Kopeček group for *A* and *B* portions are listed below, though there exists inherent mutability to these sequences, allowing for potential customization of a triblock hydrogel's biophysical properties in downstream applications (Reprinted with permission from Kopeček et al. (2007) Copyright 2007 *Biomaterials*)

copolymers is their reversibility, wherein virtual cross-links resultant from the coiled-coil interactions can be reversibly denatured, yielding a gel to sol transition. However, the A blocks retain the capacity to re-form the coiled-coil structure upon removal of the denaturing conditions. Moreover, the interaction between helices is highly tunable; minute changes in sequence, especially to the alpha helical regions can produce discernible effects on the biophysical properties of the resultant morphologies (Kopeček 2007). Xu and Kopeček noted that the physical characteristics of their ABA triblock and AB diblock hydrogels depended on the relative lengths of the A block and B block, the sequence composition, and the introduction of specific electrostatic interactions. Tirrell and co-workers programmed further specificity into these systems through diversification of the polypeptide sequence to create an ABC triblock system. In this architecture, the A and C domains comprise different coiled-coil sequences that exhibit little tendency to associate heteromerically, that is, the A and C blocks are structurally orthogonal (Shen et al. 2006). The presence of these orthogonal coiled-coil sequences inhibits the formation of intramolecular loops, which were prevalent within hydrogels derived from the ABA triblock systems, and, consequently, lowers the rate of erosion of free polymer from the surface of the resultant hydrogel.

An additional advantage of the coiled-coil motif lies in its ability to accommodate mutations at specific positions while retaining its structural integrity (Harbury et al. 1993, 1994). As a consequence, sequences that encode biological functions can be introduced into the scaffold of the coiled-coil structural units. This structural robustness enabled Huang et al. to implant the RGD domain between two hexaheptad sequences (A2) derived from a previously published leucine zipper (LZ) coiled-coil peptide. The RGD domain was separated from each A2 sequence by a nine amino acid spacer (C1). A *C*-terminal tail (C2), containing cysteine, was also added, completing an RGD-containing system constructed as follows: A2-C1-

RGDS-C1-A2-C2. The insertion of RGDS imbued cell adhesion to the hydrogel (Huang et al. 2014). Specifically, Huang et al. found that RGD sequences introduced into LZ hydrogels promoted the attachment (as determined via MTS cell proliferation assay kit, a colorimetric analysis which measures the reduction of 3-(4,5-dimethylthiazol-2-yl)-5-(3-carboxymethoxyphenyl)-2-(4-sulphophenyl)-2H-tetrazolium, or MTS) and proliferation of metabolically active cells at quantitatively higher levels than the control system: A2-C1-C1-A2-C2, which lacked the RGD domain. These results were corroborated *in vivo* using human marrow stem cells in a murine host system, which demonstrated cell attachment, growth and even neovascularity, thus proving that a mutable, tunable, coiled-coil-based hydrogel has potential for tissue engineering applications (Huang et al. 2014). This "customization" of a hydrogel is possible primarily due to the structural stability encoded within the coiled-coil LZ domain, and its ability to incorporate mutations near it without loss of its structure/function relationship.

Hybrid hydrogels are derived from self-assembly of synthetic polymers to which coiled-coil sequences have been covalently attached, usually at the termini, to afford ABA-type protein-polymer conjugates (Kopeček 2007). These hybrid materials combine the specificity of coiled-coil interactions with the well-known mechanical properties and biocompatibility of synthetic biomaterials. Kopecek and Yang (2012) linked *N*-(2-Hydroxypropyl) methacrylamide (HPMA) to (N',N'-dicarboxymethylaminopropyl) methacrylamide (DAMA) to create a copolymer that served as the main polymer component of the hydrogel. The HPMA polymer, a hydrophilic molecule, promotes the water absorption and swelling of the hydrogel. DAMA, a metal-chelating agent, provided a mechanism to couple the polymer chain to the peptide moiety of the hydrogel via Ni^{2+} chelation between DAMA and a His-tag domain within the peptide. The HPMA-DAMA copolymer was conjugated to two differing coiled-coil-forming peptide sequences with differing lengths and amino acid compositions: CC1 and CC2. CC1 was derived from a portion of the stalk domain of kinesin, adopting a tetrameric coiled-coil structure. In contrast, CC2 was designed by the Kopeček group as a tetrameric coiled-coil, but comprised a shorter sequence than CC1. Importantly, it was observed that CC2 exhibited greater thermostability than CC1. These investigators hypothesized that differences in amino acid sequence between the two coiled-coil motifs (CC1 and CC2) would produce measurable effects in subsequent downstream biophysical properties. The difference in sequence between CC1 and CC2 influences the thermodynamic stability of the resulting coiled-coils, which, in turn, would affect the properties of the resultant hydrogel. For example, the T_m of a coiled-coil could be raised or lowered through sequence control, which enabled the formation of hydrogels of varying thermostability. When subjected to a temperature increase from 25° to 70 °C, the CC1-based hydrogel volume decreased tenfold (Wang et al. 1999). The mid-point temperature of the gel-sol transition coincided with the T_m of the constituent coiled-coil that was determined from its CD melting transition. Conversely, CC2 did not exhibit a hydrogel volume transition within the same temperature range (Wang et al.

1999). Kopeček asserted that this data indicated that "properties of a well-defined coiled-coil protein motif can be imposed onto a hybrid hydrogel" (Kopeček 2007).

In the pursuit of enhanced stability and a dynamic mechanical response, Yao et al. created a hybrid hydrogel that incorporated reversible physical cross-links and photo-polymerizable groups (Yao et al. 2014). A reactive cysteine residue was introduced into the sequence of a coiled-coil derived from the five-helix bundle of cartilage oligomeric matrix protein (COMP). The COMP peptide was conjugated to a macromer of polyethylene glycol diacrylate (PEGDA) through Michael addition to one of the terminal acrylate groups. The resultant pentameric assembly contained PEG chains that were terminally functionalized with the remaining acrylate group. Photo-induced polymerization of the terminal acrylates afforded a network in which the pentameric coiled-coil acted as a physical cross-link between polymer chains. This process has the advantage of retaining the dynamic physical cross-links associated with the coiled-coil motif, while permitting rapid *in situ* fabrication of the hydrogel using photo-induced polymerization (Yao et al. 2014). Fibroblast cells could be encapsulated within a 3D hydrogel matrix, which was generated *in situ* via photo-polymerization of an RDG-modified peptide-macromer. The reversibility of the coiled-coil self-association enabled self-healing behaviour within the hydrogel, which promoted cell spreading and migration in 3D culture (Yao et al. 2014). These hydrogel systems demonstrate a key advantage in the use of coiled-coils as structural units within self-assembling biomaterials, namely the potential for customization of the selectivity and stability of the interaction.

In the cases described above, the coiled-coil was employed primarily as a biorecognition motif in order to create the virtual cross-links that defined the hydrogel. The hydrophilic central block provided the flexibility to accommodate the swelling solvent. However, Woolfson and co-workers demonstrated hydrogels could be created solely from α-helical peptide sequences, which they termed hydrogelating self-assembling fibres (hSAFs) (Banwell et al. 2009). The hSAF system is based on previous work performed by the Woolfson group, wherein they engineered self-assembling fibres (SAFs) via two α-helices co-assembling such that the resultant structure was a dimer of the two helices. Importantly, this dimer featured sticky ends, and resultant end-to-end assembly produced coiled-coil fibrils, which in turn aggregated to form large fibres. It was observed that these fibres demonstrated a high level of order, leading to their precipitation from solution (Banwell et al. 2009). Using the SAF as a starting scaffold, the researchers inserted alanine residues (to encourage hydrophobic interactions between fibrils) and glutamine residues (to promote hydrogen bonding). These mutations were performed only at the *b, c*, and *f* positions of the heptad repeat, as these lie on the exposed surface of the helix, while other residue positions are more critical in driving dimerization of the two constituent helices to form a coiled-coil. Differing levels of alanine and glutamine were introduced at the aforementioned positions to form hydrogels driven largely by hydrophobic interactions between fibrils or driven by hydrogen bonding. It was observed that the hydrophobically-driven hydrogels (those featuring proportionally large amounts of alanine at the variable positions) showed an increase in gel strength

when heated. Conversely, the hydrogel variants driven primarily by hydrogen bonding (those featuring proportionally large levels of glutamine at the variable positions) melted and lost their gel strength upon heating. A distinct advantage of this system is that each constituent helix has its own sequence identity, and hydrogelation only occurs upon mixing. Lastly, Woolfson and co-workers showed that these hSAF systems are compatible with, and support both cell growth and cell differentiation. A recurring theme regarding coiled-coil biomaterials is the flexibility of this protein fold as a structural platform. Mehrban et al. demonstrated that these fibrillar coiled-coils could be decorated with the RGDS cell-adhesive sequence. The resultant hydrogels could promote the growth, directional migration, and differentiation of murine embryonic neural stem cells in culture (Banwell et al. 2009; Mehrban et al. 2015).

17.4 Immunogenic Coiled-Coil Assemblies

An important factor to consider in the development of biomaterials for *in vivo* applications is immunogenic response. For tissue engineering applications, minimizing the immune response to the coiled-coil construct facilitates integration into the body with minimal risk of rejection. In contrast, immunotherapies rely on a strong immune response to the coiled-coil material (Boato et al. 2007). It follows that it is of great interest to not only measure the immunogenic potential of coiled-coil assemblies under physiologically relevant conditions for *in vivo* applications, but also to design systems in which immunological response can be controlled.

For a biomaterial to provoke an immune response, it must interact with the immune system either by being recognized as a foreign body or by breaking down the native B-cell tolerance (if it is sufficiently homologous to a protein in the host organism). In both cases, aggregated (Maas et al. 2007) or oligomerized (Rosenberg 2008) proteins have been shown to be more immunogenic than their monomeric counterparts. Biomaterials that do not provoke an immune response are invisible to the host cell and function freely within the cell. Because coiled-coil systems can access a variety of oligomeric states, they are ideal for tuning an immune response.

Recently the Collier group explored the effect of PEGylation on the immunogenicity of coiled-coil assemblies. PEGylation generally reduces immune response, while aggregation increases the immune response (Rudra et al. 2010a). The interesting question then, is how strong will the immune response be when a PEGylated peptide aggregates? To address this question, they investigated the murine immune response to three peptides: a domain from mouse fibrinogen (which disfavours coiled-coil formation due to poor charge pairings and buried polar residues), a mutated version of the same with a coiled-coil optimized sequence (γKEI), and a triblock peptide-polymer conjugate (γKEI-PEG-γKEI) (Rudra et al. 2010b). They found that the native peptide and its coiled-coil derivative elicited no immune response, while the triblock peptide copolymer caused a mild immune response.

They attributed this change in immune response to the higher degree of oligomerization observed in the triblock copolymer, as determined from analysis using analytical ultracentrifugation (AUC). These results suggested that the immunogenicity of the peptide was not based on the folding, as the native random coil peptide and the coiled-coil forming mutant elicited similarly low immune responses.

In a particularly interesting study, the Burkhard group developed a coiled-coil nanoparticle with antiviral properties against Severe Acute Respiratory Syndrome (SARS) (Pimentel et al. 2009). SARS is a pneumonia-like disease that caused widespread concern in 2002, when it rapidly spread among 29 different countries and resulted in the deaths of 800 people (Marra et al. 2003; Nicholls et al. 2003). The epicentre of this outbreak was in southern China, where several domesticated animal species were found to be carrying the disease in live animal markets (Guan et al. 2003). The search for a SARS vaccine resulted in the identification of the SARS corona virus S protein. Attempts to use the full-length S protein to vaccinate different model animals resulted in increased virulence of hepatitis in ferrets (Czub et al. 2005) and infection with SARS in cats (Corapi et al. 1992). Thus, the design of an S protein B cell epitope became an important research target. The key to designing an effective epitope is mimicking the native protein structure; because of this consideration, the coiled-coil forming region of the S protein was used as the vaccine nanoparticle scaffold (Raman et al. 2006). They were able to develop a monomer that would self-assemble into a viral capsid-mimicking icosahedral nanoparticle (Fig. 17.5). The coiled-coil assembly had the advantages of high stability, ease of expression, and lack of infectivity seen in the full S protein. In addition, the coiled-coil assembly was found to be highly immunogenic due to its size, mimicry of the native epitope, and repetitive epitope display, making it a reasonable first step to developing a SARS vaccine.

17.5 Coiled-Coil Based Nanotubes, Fibrils, and Fibres

One-dimensional assemblies derived from proteins and peptides have been the focus of significant scientific research over the last two decades (Scanlon and Aggeli 2008). A significant motivation for this research stems from the presence of extended helical assemblies in native biological systems, in which they display a variety of functional roles that would be desirable to replicate within synthetic biomaterials. The knobs-into-holes packing typically associated with coiled-coils has been observed to play a significant role in stabilizing the structures of helical assemblies such as intermediate filaments (Chernyatina et al. 2015), type IV pili (Craig et al. 2006), bacterial flagella (Yonekura et al. 2003), the type III secretion system needle complex (Loquet et al. 2012), and filamentous phage capsids (Morag et al. 2015). Significant research effort has been directed toward the *de novo* design of helical assemblies based on coiled-coil structural motifs, which could be employed for the creation of synthetic scaffolds for biomedical applications (see above, for example).

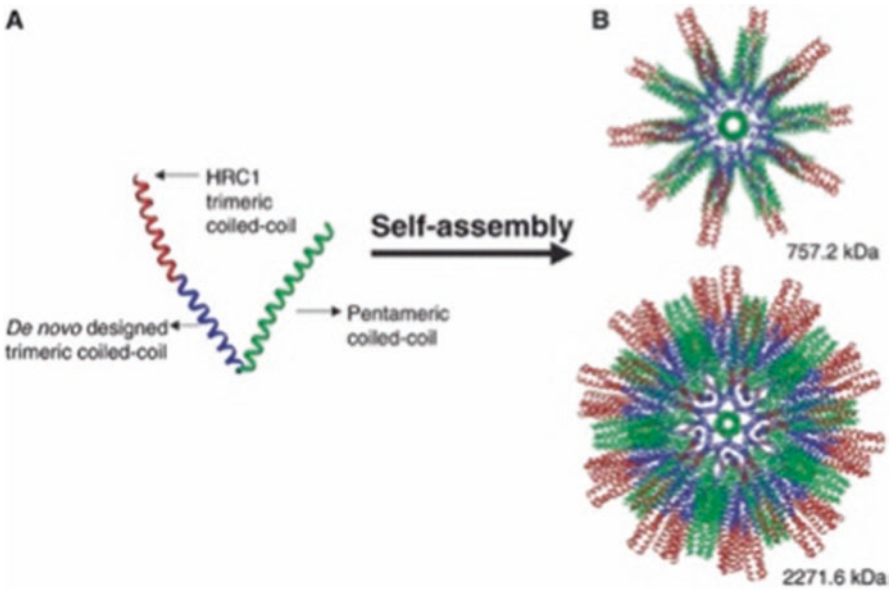

Fig. 17.5 Design of the icosahedral coiled coil epitope as a potential SARS vaccine. (**a**) the HRC1 domain and self assembly partners. (**b**) A 60 unit icosahedral assembly of the peptide nanoparticle (*top*) and a larger 180 unit icosahedral form (*bottom*) (Reprinted from Pimentel et al. (2009) Copyright 2009 *Chem Biol Drug Des*)

The primary approach of this research focused on design of sticky-ended coiled-coils that could oligomerize to form infinite one-dimensional polymers through non-covalent interactions. The staggered alignment of helices was promoted through introduction of electrostatic interaction between helical protomers that enforced an out-of-register alignment across the helical interface. However, most designs focused on coiled-coils of lower oligomerization state (usually dimers and trimers), primarily due to the difficulty in controlling alignment between adjacent helices for coiled-coils in larger helical bundles. In addition, at that juncture, limited structural information was available on coiled-coils of higher oligomerization state. One attractive feature of the latter systems is that coiled-coils of oligomerization state ≥ 5 helices display an interior channel in which the diameter depends on the bundle size. Self-assembly of coiled-coils of higher oligomerization state affords the potential to create nanotube structures in which the channel residues can be tailored for encapsulation of small molecules and the outer surface can be functionalized to enhance applications such as selective targeting for controlled release.

Numerous strategies have been described to drive the formation of tubular assemblies from peptides and proteins, though few of these approaches are applicable to coiled-coil systems (Burgess et al. 2015). The most promising approach to nanotube fabrication involves the end-to-end stacking of coiled-coils of defined oligomerization state ($n \geq 5$) into extended structures through selective introduction of attractive non-covalent interactions at the interfaces between subunits. As

coiled-coils are perhaps the best understood protein fold, with a wealth of available structural information, they represent a promising test bed to develop methods to reliably generate structurally-defined supramolecular assemblies.

Xu et al. (2013) described an approach to promote the end-to-end self-assembly of a seven-helix bundle into a helical nanotube. These researchers employed a structurally characterized 7-helix bundle, GCN4-pAA, as the starting point for the design. In this case, the 7-helix bundle has helical symmetry, in that successive peptides in the assembly are axially translated by an increment of one residue (1.43 Å rise per residue for the superhelix) between successive helices in the bundle. This translation results in a registry shift corresponding to a heptad repeat between the first and last helix in the bundle. The corresponding edges at the *N*- and *C*-termini are solvent-exposed and, upon interaction, could bury sufficient hydrophobic surface area to promote stacking of the 7-helix bundles. Xu et al. (2013) used the analogy of a helical lock washer to describe the structure of the coiled-coil subunits. The sequence of GCN4-pAA was redesigned to afford a fibrillogenic peptide sequence, 7HSAP1. This sequence preserved the residues that were critical for formation of the 7-helix bundle, but introduced features that would promote stacking of the subunits (Xu et al. 2013). Hydrophobically-driven association of complementary helix faces yielded a non-covalent assembly of helices with an inner lumen. In addition, the *N*-terminus and *C*-terminus of 7HSAP1 were populated with positively charged residues and negatively charged residues, respectively. This design promoted charge complementary association of helical heptamers through head-to-tail stacking of the heptameric subunits. The resultant nanotubes defined an internal cavity of approximately 7 Å in diameter, in analogy with the crystal structure of GCN4-pAA, which was capable of binding shape-appropriate small molecules such as the solvatochromic fluorophore PRODAN (Xu et al. 2013).

Hume et al. constructed a fibrillar assembly using the pentameric coiled-coil region of cartilage oligomeric matrix protein (COMPcc) as the basis for design. A variant of COMPcc was constructed in which residues that were non-essential for pentameric assembly were deleted (Hume et al. 2014). An *N*-terminal pocket, inherent to the wild type matrix protein and consisting of three leucines and a valine, was shifted with respect to the overall sequence, but preserved in identity and conserved with respect to its occurrence within the heptad repeat sequence. The presence of the *N*-terminal pocket was necessary to retain the preference for the pentameric assembly (over alternative oligomeric states or lack of assembly). Moreover, in the re-designed peptide, Q, charge density was introduced at positions on the outer (lateral) surface of the assembly in order to promote complementary interactions between oppositely charged regions on adjacent pentameric assemblies. Fibre formation would be promoted through head-to-tail stacking of helical bundles, which would be reinforced through lateral association between fibrils mediated through electrostatic complementarity. Peptide Q was found to form nano-fibres having diameters as large as half a micron (Hume et al. 2014). The pentameric assembly also defined a central pore of sufficient size to accommodate small molecules, such as the therapeutic agent curcumin. Curcumin was demonstrated not only to bind to

the fibrillar assemblies, but also to promote further lateral association through a mechanism that has yet to be fully elucidated. Using this approach, Hume et al. succeeded in engineering the first documented experimentally-assembled protein-based microfibre, observing diameters of up to sixteen microns via aggregation of nano-scale moieties, while preserving a central cavity for encapsulation (Hume et al. 2014).

Burgess et al. recently described a more general approach to the design of fibrils, including nanotubes, derived from coiled-coil sequences having different oligomerization states (Burgess et al. 2015). Helical bundles of defined oligomerization state ranging from three to seven were designed, in which residues at the *N*- and *C*-termini were chosen to be electrostatically complementary in charge (as described above). This design element was introduced to promote end-to-end association of coiled-coil bundles, affording one-dimensional assemblies from blunt-ended stacking of helical bundles. The resultant sequences (termed CC-Tri through CC-Hept), self-assembled into fibrils based on subunits having the corresponding oligomerization state, albeit with differing degrees of lateral association and order (Fig. 17.6). One system, CC-Hex-T, based on a hexameric helical bundle, exhibited a high degree of para-crystalline order after thermal annealing in PBS buffer. Burgess et al. further demonstrated that the hydrophobic dye 1,6-diphenylhexatriene was able to penetrate and bind within the inner lumen of tubular assemblies derived from CC-Hex-T, but not to the fibres derived from the tetrameric bundle CC-Tet2-F (Burgess et al. 2015). Subsequent experiments established that dye binding only occurred for helical bundles having an oligomerization state from 5–7, as these larger coiled-coil subunits define an inner lumen of sufficient size to accommodate the guest molecule. The encapsulation of 1,6-diphenylhexatriene validates the potential of these tubular materials for applications involving drug or small molecule binding and release.

While larger coiled-coil bundles (>7 subunits) have been observed in native protein assemblies, the *de novo* design of larger diameter coiled-coils remains a challenge, which has thus far limited the fabrication of nanotubes with larger lumens. Walshaw and Woolfson (Walshaw and Woolfson 2001) described general principles for design of these types of assemblies based on an analysis of the 12-helix bundle observed in the structure of the tolC homotrimer (Koronakis et al. 2000). However, such large diameter tubular structures based on coiled-coils have yet to be realized. Egelman et al. (2015) investigated the self-assembly of a pair of *de novo* designed coiled-coils based on the structural principles proposed by Walshaw and Woolfson. The sequences of these two peptides were based on a canonical heptad repeat motif in which hydrophobic residues populate the *a/d* and *c/f* positions, producing hydrophobic seams along the helix offset by two residue spacing (Koronakis et al. 2000). In contrast to the α-helical cylinder of the tolC sequence (Calladine et al. 2001) hydrophobic residues at the outer *a* and *f* positions were substituted with alanines, which feature smaller sidechains than the residues of the native tolC. This substitution served to decrease steric interference between the flanking residues of the two hydrophobic pockets to encourage larger tube diameter (Egelman et al. 2015). Large sidechains at the outer positions would create steric interactions between neigh-

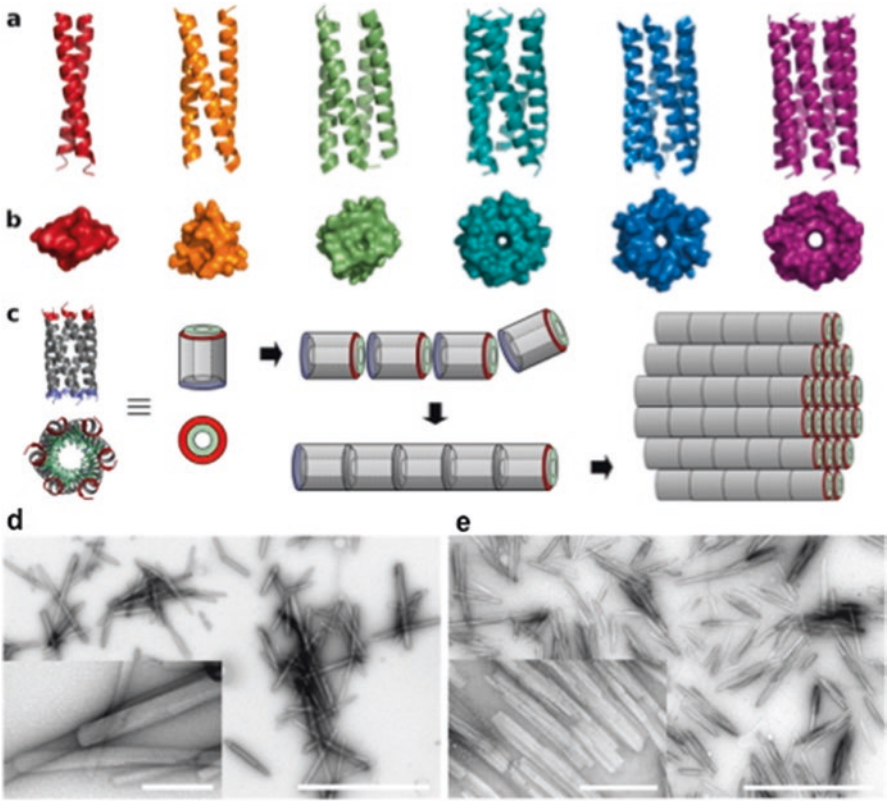

Fig. 17.6 [*top*] X-ray crystal-derived graphical representations of CC-Di through CC-Hex. [*bottom*] Transmission electron micrographs of tube assemblies (**a**) Graphical representation of coiled-coil oligomers ranging from two to seven, indicating the overall structure of the coiled-coil subunit as seen side-on. (**b**) X-ray crystal-derived graphical representations of coiled-coil oligomers ranging from two to seven indicating the overall structure of the coiled-coil subunit as seen when viewed along the fibre axis. In the pentamer, hexamer, and heptamer assemblies, a putative inner lumen is observed. (**c**) Putative method of assembly of coiled-coil subunits, wherein end-to-end association drives fibre formation. (**d**) Transmission electron micrographs of negative stained CC-Tet. (**e**) Transmission electron micrographs of CC-Pent (Reprinted with permission from Burgess et al. (2015) Copyright 2015 *J Am Chem Soc*)

bouring residues, and in the relaxation and mitigation of this steric stress, force the tube to constrict towards a smaller diameter. This was negated in the synthetic peptide via mutations to alanine at the aforementioned heptad positions *a* and *f* to encourage large diameter growth. Moreover, complementary pairs of charged residues populate the *b* and *e* positions in the synthetic peptide to promote antitypic helix-helix association (Egelman et al. 2015). The sole difference between the two sequences was the substitution of four arginine residues in the first peptide (Form I) with four lysine residues in the second peptide (Form II). Both peptides formed

extended tubular assemblies in aqueous buffer, but differed significantly in diameter (6 nm for the Form I assemblies and 12 nm for the Form II assemblies).

Electron cryomicroscopy with direct electron detection was employed for the structural analysis of the Form I and Form II assemblies. Egelman et al. (2015) funnelled data through the iterative helical real space reconstruction algorithm (Egelman 2010) to produce near atomic resolution structural data for Forms I and II. Form I features a unilaminar helical motif, wherein helices are packed nearly perpendicular to the nanotube axis in which the cross-section displays near four-fold symmetry in the left-handed one-start helix. The Form II assemblies feature a bilaminar helical motif, wherein three bilayer stacks of helices are packed together and define a nearly circular cross-section in which the helices are slightly inclined with respect to the cross-sectional plane. In either structure, the nanotube lumen and outer surface are lined with functional groups from polar amino acid residues. One might envision that the inner and outer surfaces of the tubes could be selectively functionalized to promote applications in controlled encapsulation and release.

Notably, the structures of the Form I and II assemblies diverged significantly from the structural model proposed by Walshaw and Woolfson, as well as that of the tolC α-cylinder (Koronakis et al. 2000; Calladine et al. 2001; Egelman et al. 2015). More remarkably, the structurally-conservative substitution of arginine for lysine resulted in significant differences in structure between the two helical assemblies. These differences highlighted a potential problem in the design of such assemblies, namely, that quaternary structure may not be robust in sequence space. Indeed, Egelman et al. demonstrated that a single mutation (R13K) was sufficient for conversion of the Form I assembly to the Form II assembly (Fig. 17.7). Conversely, a coupled pair of mutations (K13R, K17R) provides for conversion of Form II assembly to the Form I assembly (Egelman et al. 2015). These structural differences are manifested as a consequence of different local interactions between subunits that are propagated hierarchically to form the two distinct assemblies. The Form I assembly derives its stability from the interaction of the sidechains of Arg13 and Arg17 with the C-terminal residues of a helix in an adjacent stack. These interactions form the corners of the fourfold symmetric cross-section of the tubular assembly. In contrast, the helical stacks of Form II assembly, lacking these structural critical arginine residues, are held together weakly through interactions between the termini of helices in adjacent stacks. The structural changes that occur as a consequence of mutagenesis can be understood in terms of abrogation or introduction of these arginine-derived interactions (Egelman et al. 2015). The difference between the Form I and Form II assemblies dramatically illustrates that variations in primary sequence can result in large changes in quaternary structures. Atomic resolution structural information enables the identification of these critical interactions that underlie these differences, but the development of coiled-coils with high oligomerization state as biomaterials will require better methods to reliably design higher order structure.

In addition to tubular assemblies, coiled-coils have been employed in the fabrication of capsular and film-like biomaterials, which have advantages as carriers for encapsulation and controlled release of drugs and other small molecules. Utilizing

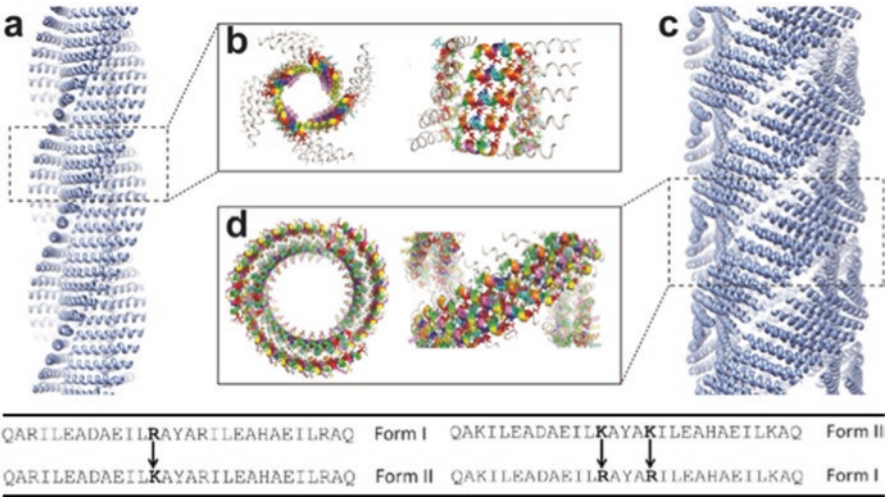

Fig. 17.7 [*top*] Atomic models for knobs-into-holes packing SOCKET analysis for Form I and Form II. [*bottom*] Sequences of Form I and II, illustrating the mutations required for interconversion between forms. (**a**) Graphical representation of atomic model for Form I via SOCKET analysis. (**b**) Graphical representation of knobs-into-holes packing of the C-terminus of Form I as seen [*left*] from along the fibre axis and [*right*] as seen from a side-on view. (**c**) Graphical representation of atomic model for Form II via SOCKET analysis. (**d**) Graphical representation of knobs-into-holes packing in Form II as seen [*left*] from along the fibre axis and [*right*] as seen from a side-on view. KIH packing is evidenced only within the same wall, and KIH packing does not occur between the two lumen (*inner* and *outer*) of the tube [(Egelman et al. 2015)] (Reprinted with permission from Egelman et al. (2015) Copyright 2015 *Structure*)

a layer-by-layer (LbL) approach, Gormley et al. have been able to construct capsules and films by subsequent addition of layers in a sequential manner (Gormley et al. 2015). Traditionally, deposition of sequential layers was achieved via self-assembly that was mediated through electrostatic complementarity between layers (Hammond 1999; Ai et al. 2003). Since this discovery, alternative means for LbL deposition have been accomplished in an effort to imbue enhanced levels of customization and specificity with respect to biophysical properties of the assembly. The LbL toolbox contains other methodologies such as hydrogen bonding, covalent bonding, DNA-based oligomerization, and streptavidin-biotin complementarity (Mart et al. 2006). Stevens and co-workers have added a new methodology to the toolkit by using the specificity inherent in the self-assembly of coiled-coil moieties (Gormley et al. 2015). Using helix-loop-helix motifs (JR2EC and JR2KC) that oligomerize as a coiled-coil tetramer, these researchers created a polymer-peptide hybrid by conjugation of cysteine to *N*-(2-hydroxypropyl)methacrylamide-*co*-*N*-(3-aminopropyl)-methacrylamide [HPMA-*co*-APMA] polymer through a 4-(*N*-maleimidomethyl) cyclohexanecarboxylic acid *N*-hydroxysuccinimide ester [SMCC] linker (Gormley et al. 2015). The linkage moiety was attached to C22 at the loop region of the helix-loop-helix. Peptides JR2EC and JR2KC differ in sequence by a total of eight glutamates/lysines, which imbued a difference in net

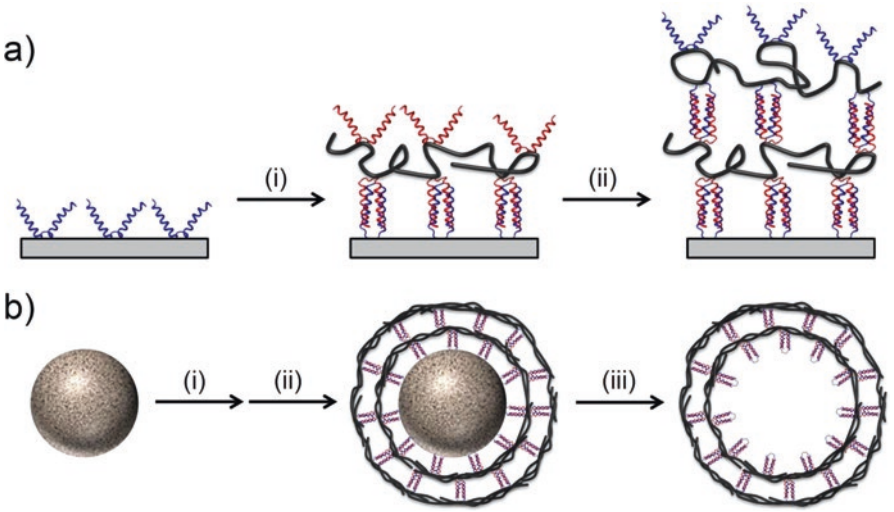

Fig. 17.8 Graphical representations of (**a**) planar LbL assembly and (**b**) spherical, colloidal LbL assembly. Tetramer coiled-coil formation drives the sequential peptide-polymer assembly of each layer (Reprinted with permission from Gormley et al. (2015) Copyright 2015 *Chem Mater*)

charge to each variant. This duality in charge promotes selective heteromerization of the two helix-loop-helix moieties, JR2EC and JR2KC, to form a tetrameric coiled-coil. As the peptide helices are conjugated to a polymer scaffold, coiled-coil formation results in sandwich-like constructions of iterative layers by sequential addition of polymer-peptide units with opposite charges. Anchoring techniques could be implemented to grow these LbL assemblies on both planar and spherical, colloidal substrates, giving a degree of geometric variation to what can be accomplished via this approach (Fig. 17.8). Lastly, as with many coiled-coil-based systems, a pH-induced conformational switch can be actuated. At pH 7, the dimer subunits stack against one another in the film. At pH 4, positive charges dominate the surface and the dimers repel one another, causing dissociation of the stacked units (Gormley et al. 2015).

17.6 Coiled-Coil Composites

This review has largely focused largely on developments related to the potential of coiled-coils for applications in biomedicine, and, specifically, their interactions with other biological materials *in vitro* or *in vivo*. Recently, however, significant research has been focused on integrating inorganic materials with coiled-coil biomaterials. In particular, the use of coiled-coils has been proposed for applications involving the templating of inorganic materials. For example, numerous studies have used genetically engineered viral capsids for directing the deposition of inorganic materials,

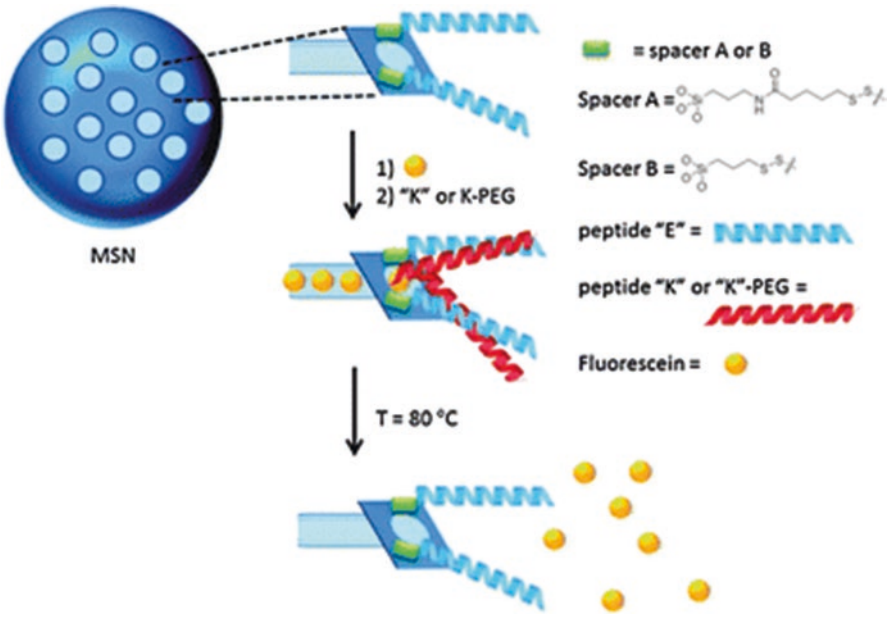

Fig. 17.9 A schematic representation of the mesoporous silica nanoparticle (MSN) system. The MSN construct is depicted in *blue*, with the small pores indicated by *light blue*. Spacers (*green squares*) of varying length are conjugated to the "E" peptide (*blue ribbon*), allowing it the flexibility needed to cover the pores. Addition of peptide "K" (*red ribbon*) leads to the sealing of the pore upon heterodimerization. Temperature increase leads to the unwinding of the coiled-coil, resulting in cargo (*yellow spheres*) delivery (Reprinted from Martelli et al. 2013)

leading to the formation of highly ordered inorganic structures (Lee et al. 2002; Huang et al. 2005). These strategies have produced very efficient electron-capture devices (Dang et al. 2011), as well as highly functioning lithium batteries (Lee et al. 2009). While using a phage capsid is an elegant solution to the selection problem, a coiled-coil scaffold would be preferable due to its ease of production, robust structure, and well-known design rules. Several examples have been recently published in which coiled-coils, or assemblies derived from their self-association, have been employed to direct nanoparticle synthesis and assembly (Ryadnov 2006; Slocik et al. 2007; Wagner et al. 2009; Hume et al. 2015; Abram et al. 2016). These materials might ultimately find use as imaging agents or therapeutics in medical applications, especially as they could leverage the favourable electronic, optical, or magnetic properties of the inorganic nanoparticle and the structural specificity of the coiled-coil interaction (Seo et al. 2015).

This objective was realized in a particularly innovative biomaterial design based on a coiled-coil composite. Martelli et al. developed a hybrid system that consisted of a coiled-coil heterodimer, fluorescein cargo, and mesoporous silica nanoparticles (Fig. 17.9) (Martelli et al. 2013). Briefly, mesoporous silica nanoparticles encapsulating large quantities of fluorescein were fabricated and conjugated to an acidic

coiled-coil peptide E. These complexes were then incubated overnight with the complementary basic coiled-coil peptide K, which was free in solution. The E and K peptides underwent selective heterodimerization, which resulted in *de facto* closure of the silica pores. The coiled-coil dimer could essentially perform as a valve, which could be actuated through denaturation of the dimer. For example, thermolysis of these complexes induced denaturation of the coiled-coil dimer. Dissociation of the K peptide actuated the valves and resulted in release of the cargo. Fluorescein was selected as a model cargo due to its fluorescent properties and ease of imaging. These materials have considerable potential for *in vivo* applications, especially if this approach proves to be more general. For example, ferromagnetic iron oxide nanoparticles would enable targeting to a specific location, e.g., a tumour, using an externally applied magnetic field. Once in the correct location, the cargo, e.g., a cytotoxic drug molecule could be released via localized heating in which the temperature leads to thermal denaturation of the heterodimeric coiled-coil.

17.7 Conclusion

Recent technological advances, such as structurally predictive computational algorithms and higher resolution characterization techniques, are expanding our ability to design and structurally characterize novel coiled-coil assemblies. The availability of this information has facilitated the development of novel biomaterials scaffolds based on coiled-coils. The natural abundance and structural diversity of coiled-coils, as well as their well-understood design rules, make them an obvious choice for biomaterials scaffolding. In addition, the versatility of the coiled-coil motif allows for the incorporation of artificial amino acids, which enhances the ability to do site-specific chemistry and generate more complex materials. As a result, coiled-coils have been used to develop a variety of structures, including hydrogels, nanotubes, nanosheets, and even composite materials with synthetic polymers or inorganic nanoparticles. Given the ever-increasing need for tailored materials, coiled-coils are emerging as a highly modular scaffold capable of a wide variety of functions.

References

Abram SB, Aupič J, Dražićd G, Gradišar H, Jerala R (2016) Coiled-coil forming peptides for the induction of silver nanoparticles. Biochem Biophys Res Commun 472(3):566–571

Ai H, Jones SA, Lvov YM (2003) Biomedical applications of electrostatic layer-by-layer nanoassembly of polymers, enzymes, and nanoparticles. Cell Biochem Biophys 39:23–43

Anzini P, Xu C, Hughes S, Magnotti E, Jiang T, Hemmingsen L, Demeler B, Conticello VP (2013) Controlling self-assembly of a peptide-based material via metal-ion induced registry shift. J Am Chem Soc 135(28):10278–10281

Apostolovic B, Deacon SPE, Duncan R, Klok H-A (2010) Hybrid polymer therapeutics incorporating bioresponsive, coiled coil peptide linkers. Biomacromolecules 11:1187–1195
Apostolovic B, Deacon SPE, Duncan R, Klok H-A (2011) Cell uptake and trafficking behavior of non-covalent, coiled-coil based polymer-drug conjugates. Macromol Rapid Commun 32:11–18
Assal Y, Mizuguchi Y, Mie M, Kobatake E (2015) Growth factor tethering to protein nanoparticles via coiled-coil formation for targeted drug delivery. Bioconjug Chem 26:1672–1677
Banwell EF, Abelardo ES, Adams DJ, Birchell MA, Corrigan A, Donald AM, Kirkland M, Serpell LC, Butler MF, Woolfson DN (2009) Rational design and application of responsive alpha-helical peptide hydrogels. Nat Mater 8:596–600
Boato F, Thomas RM, Ghasparian A, Freund-Renard A, Moehle K, Robinson JA (2007) Synthetic virus-like particles from self-assembling coiled-coil lipopeptides and their use in antigen display to the immune system. Angew Chem Int Ed Eng 46:9015–9018
Burgess NC, Sharp TH, Thomas F, Wood CW, Thomson AR, Zaccai NR, Brady RL, Serpell LC, Woolfson DN (2015) Modular design of self-assembling peptide-based nanotubes. J Am Chem Soc 137(33):10554–10562
Calladine CR, Sharff A, Luisi B (2001) How to untwist an α-helix: structural principles of an α-helical barrel1. J Mol Biol 305(3):603–618
Chernyatina AA, Guzenko D, Strelkov SV (2015) Intermediate filament structure: the bottom-up approach. Curr Opin Cell Biol 32:65–72
Chu T-W, Kopeček J (2015) Drug-free macromolecular therapeutics – a new paradigm in polymeric nanomedicines. Biomed Sci 3:908–922
Corapi WV, Olsen CW, Scott FW (1992) Monoclonal antibody analysis of neutralization and antibody-dependent enhancement of feline infectious peritonitis virus. J Virol 66:6695–6705
Craig L, Volkmann N, Arvai AS, Pique ME, Yeager M, Egelman EH, Tainer JA (2006) Type IV pilus structure by cryo-electron microscopy and crystallography: implications for pilus assembly and functions. Mol Cell 23(5):651–662
Czub M, Weingartl H, Czub S, He R, Cao J (2005) Evaluation of modified vaccinia virus ankara based recombinant SARS vaccine in ferrets. Vaccine 23:2273–2279
Dang X, Yi H, Ham MH, Qi J, Yun DS, Ladewski R, Strano MS, Hammond PT, Belcher AM (2011) Virus-templated self-assembled single-walled carbon nanotubes for highly efficient electron collection in photovoltaic devices. Nat Nanotechnol 6:377–384
Dublin SN, Conticello VP (2008) Design of a selective metal ion switch for self-assembly of peptide-based fibrils. J Am Chem Soc 130:49–51
Egelman EH (2010) Reconstruction of helical filaments and tubes. Methods Enzymol 482:167–183
Egelman EH, Xu C, DiMaio F, Magnotti E, Modlin C, Yu X, Wright E, Baker D, Conticello VP (2015) Structural plasticity of helical nanotubes based on coiled-coil assemblies. Structure 23(2):280–289
Elisseeff J (2008) Hydrogels: structure starts to gel. Nat Mater 7(4):271–273
Fletcher NL, Lockett CV, Dexter AF (2011) A pH-responsive coiled-coil peptide hydrogel. Soft Matter 7(21):10210–10218
Frampton JP, Hynd MR, Shuler ML, Shain W (2011) Fabrication and optimization of alginate hydrogel constructs for use in 3D neural cell cuture. Biomed Mater 6:18
Garbern JC, Minami E, Stayton PS, Murry CE (2011) Delivery of basic fibroblast growth factor with a pH-responsive, injectable hydrogel to improve angiogenesis in infarcted myocardium. Biomaterials 32:2407–2416
Gormley AJ, Chandrawati R, Christofferson AJ, Loynachan C, Jumeaux C, Artzy-Schnirman A, Aili D, Yarovsky I, Stevens MM (2015) Layer-by-layer self-assembly of polymer films and capsules through coiled-coil peptides. Chem Mater 27(16):5820–5824
Grigoryan G, Degrado WF (2011) Probing designability via a generalized model of helical bundle geometry. J Mol Biol 405(4):1079–1100

Gruber M, Lupas AN (2003) Historical review: another 50th anniversary – new periodicities in coiled coils. Trends Biochem Sci 28(12):679–685

Guan Y, Zheng BJ, He YQ, Liu XL, Zhuang ZX, Cheung CL, Luo SW, Li PH, Zhang LJ, Guan YJ, Butt KM, Wong KL, Chan KW, Lim W, Shortridge KF, Yuen KY, Peiris JS, Poon LL (2003) Isolation and characterization of viruses related to the SARS coronavirus from animals in southern China. Science 302:276–278

Guziewicz N, Best A, Perez-Ramirez B, Kaplan DL (2011) Lyophilized silk fibroin hydrogels for the sustained local delivery of therapeutic monoclonal antibodies. Biomaterials 32:2642–2650

Hammond PT (1999) Recent explorations in electrostatic multilayer thin film assembly. Curr Opin Colloid Interface Sci 4:430–442

Harbury PB, Zhang T, Kim PS, Alber T (1993) A switch between two-, three-, and four-stranded coiled coils in GCN4 leucine zipper mutants. Science 262(5138):1401–1407

Harbury PB, Kim PS, Alber T (1994) Crystal structure of an isoleucine-zipper trimer. Nature 371:80–83

Huang Y, Chiang CY, Lee SK, Gao Y, Hu EL, De Yoreo J, Belcher AM (2005) Programmable assembly of nanoarchitectures using genetically engineered viruses. Nano Lett 5:1429–1434

Huang CC, Ravindran S, Yin Z, George A (2014) 3-D self-assembling leucine zipper hydrogel with tunable properties for tissue engineering. Biomaterials 35(20):5316–5326

Hume J, Sun J, Jacquet R, Renfrew PD, Martin JA, Bonneau R, Gilchrist ML, Montclare JK (2014) Engineered coiled-coil protein microfibers. Biomacromolecules 15(10):3503–3510

Hume J, Chen R, Jacquet R, Yang M, Montclare JK (2015) Tunable conformation-dependent engineered protein-gold nanoparticle nanocomposites. Biomacromolecules 16(6):1706–1713

Jung JP, Moyano JV, Collier JH (2011) Multifactorial optimization of endothelial cell growth using modular synthetic extracellular matrices. Integr Biol 3:185–196

Kopecek J (2007) Hydrogel biomaterials: a smart future? Biomaterials 28(34):5185–5192

Kopecek J, Yang J (2012) Smart self-assembled hybrid hydrogel biomaterials. Angew Chem Int Ed Eng 51(30):7396–7417

Koronakis V, Sharff A, Koronakis E, Luisi B, Hughes C (2000) Crystal structure of the bacterial membrane protein TolC central to multidrug efflux and protein export. Nature 405(6789):914–919

Lee SW, Mao C, Flynn CE, Belcher AM (2002) Ordering of quantum dots using genetically engineered viruses. Science 296:892–895

Lee YJ, Yi H, Kim WJ, Kang K, Yun DS, Strano MS, Ceder G, Belcher AM (2009) Fabricating genetically engineered high-power lithium-ion batteries using multiple virus genes. Science 324:1051–1055

Lin YH, Lin JH, Peng SF, Yeh CL, Chen WC, Chang TL, Liu MJ, Lai CH (2011) Multifunctional gentamicin supplementation of poly(gamma-glutamic acid)-based hydrogels for wound dressing application. J Appl Polym Sci 120:1057–1068

Loquet A, Sgourakis NG, Gupta R, Giller K, Riedel D, Goosmann C, Griesinger C, Kolbe M, Baker D, Becker S, Lange A (2012) Atomic model of the type III secretion system needle. Nature 486(7402):276–279

Lupas AN (1996) Coiled coils: new structures and new functions. Trends Biochem Sci 21(10):375–382

Lupas AN, Gruber M (2005) The structure of α-helical coiled coils. Adv Protein Chem 70:37–78

Maas C, Hermeling S, Bouma B, Jiskoot W, Gebbink MFBG (2007) A role for protein misfolding in immunogenicity of biopharmaceuticals. J Biol Chem 282:2229–2236

Marra MA, Jones SJ, Astell CR, Holt RA, Brooks-Wilson A, Butterfield YS, Khattra J, Asano JK, Barber SA, Chan SY, Cloutier A, Coughlin SM, Freeman D, Girn N, Griffith OL, Leach SR, Mayo M, Mcdonald H, Montgomery SB, Pandoh PK, Petrescu AS, Robertson AG, Schein JE, Siddiqui A, Smailus DE, Stott JM, Yang GS, Plummer F, Andronov A, Artsob H, Bastien N, Bernard K, Booth TF, Bowness D, Czub M, Drebot M, Fernando L, Flick R, Garbutt M, Gray

M, Grolla A, Jones S, Feldmann H, Meyers A, Kabani A, Li Y, Normand S, Stroher U, Tipples GA, Tyler S, Vogrig R, Ward D, Watson B, Brunham RC, Krajden M, Petric M, Skowronski DM, Upton C, Roper RL (2003) The genome sequence of the SARS-associated coronavirus. Science 300:1399–1404

Mart RJ, Osborne RD, Stevens MM, Ulijn RV (2006) Peptide-based stimuli-responsive biomaterials. Soft Matter 2(10):822

Martelli G, Zope HR, Capell MB, Kros A (2013) Coiled-coil peptide motifs as thermoresponsive valves for mesoporous silica nanoparticles. Chem Commun 49:9932–9934

Mehrban N, Zhu B, Tamagnini F, Young FI, Wasmuth A, Hudson KL, Thomson AR, Birchall MA, Randall AD, Song B, Woolfson DN (2015) Functionalized α-helical peptide hydrogels for neural tissue engineering. ACS Biomater Sci Eng 1(6):431–439

Morag O, Sgourakis NG, Baker D, Goldbourt A (2015) The NMR–rosetta capsid model of M13 bacteriophage reveals a quadrupled hydrophobic packing epitope. Proc Natl Acad Sci 112(4):971–976

Nicholls J, Dong XP, Jiang G, Peiris M (2003) SARS: clinical virology and pathogenesis. Respirology 8:6–8

Pechar M, Pola R, Laga R, Ulbrich K, Bednárová L, Maloň P, Sieglová I, Král V, Fábry M, Vaněk O (2011) Coiled coil peptides as universal linkers for the attachment of recombinant proteins to polymer therapeutics. Biomacromolecules 12:3645–3655

Petka WA, Harden JL, McGrath KP, Wirtz D, Tirrell DA (1998) Reversible hydrogels from self-assembling artificial proteins. Science 281(5375):389–392

Pimentel TA, Yan Z, Jeffers SA, Holmes KV, Hodges RS, Burkhard P (2009) Peptide nanoparticles as novel immunogens: design and analysis of a prototypic severe acute respiratory syndrome vaccine. Chem Biol Drug Des 73:53–61

Pola R, Laga R, Ulbrich K, Sieglová I, Král V, Fábry M, Kabešová M, Kovář M, Pechar M (2013) Polymer therapeutics with a coiled coil motif targeted against murine BCL1 leukemia. Biomacromolecules 14:881–889

Raman S, Machaidze G, Lustig A, Aebi U, Burkhard P (2006) Structure-based design of peptides that self-assemble into regular polyhedral nanoparticles. Nanomedicine 2:95–102

Rosenberg AS (2008) Effects of protein aggregates: an immunologic perspective. AAPS J 8:E572

Rudra JS, Tian PK, Hildeman DA, Jung JP, Collier JH (2010a) Immune responses to coiled coil supramolecular biomaterials. Biomaterials 31:8475–8483

Rudra JS, Tian YF, Jung JP, Collier JH (2010b) A self-assembling peptide acting as an immune adjuvant. Proc Natl Acad Sci U S A 107:622–627

Ryadnov MG (2006) A self-assembling peptide polynanoreactor. Angewandte Chemie Int Ed 46(6):969–972

Scanlon S, Aggeli A (2008) Self-assembling peptide nanotubes. Nano Today 3(3-4):22–30

Seo JW, Ang J, Mahakian LM, Tam S, Fite B, Ingham ES, Beyer J, Forsayeth J, Bankiewicz KS, Xu T, Ferrara KW (2015) Self-assembled 20-nm 64Cu-micelles enhance accumulation in rat glioblastoma. J Control Release 220:51–60

Shen W, Zhang K, Kornfield JA, Tirrell DA (2006) Tuning the erosion rate of artificial protein hydrogels through control of network topology. Nat Mater 5(2):153–158

Slaughter BV, Khurshid SS, Fisher OZ, Khademhosseini A, Peppas NA (2009) Hydrogels in regenerative medicine. Adv Mater 21(32-33):3307–3329

Slocik JM, Tam F, Halas NJ, Naik RR (2007) Peptide-assembled optically responsive nanoparticle complexes. Nano Lett 7(4):1054–1058

Testa OD, Moutevelis E, Woolfson DN (2009) CC+: a relational database of coiled-coil structures. Nucleic Acids Res 37(suppl 1):D315–D322

Thanasupawat T, Bergen H, Hombach-Klonisch S, Krcek J, Ghavami S, Del Bigio MR, Krawitz S, Stelmack G, Halayko A, McDougall M, Meier M, Stetefeld J, Klonisch T (2015) Platinum (IV) coiled coil nanotubes selectively kill human glioblastoma cells. Nanomedicine 11:913–925

Thompson AR, Wood CW, Burton AJ, Bartlett GJ, Sessions RB, Brady RL, Woolfson DN (2014) Computational design of water-soluble α-helical barrels. Science 346(6208):485–488

Wagner SC, Roskamp M, Cölfen H, Böttcher C, Schlecht S, Koksch B (2009) Switchable electrostatic interactions between gold nanoparticles and coiled coil peptides direct colloid assembly. Org Biomol Chem 7:46–51

Walshaw J, Woolfson DN (2001) Open-and-shut cases in coiled-coil assembly: alpha-sheets and alpha-cylinders. Protein Sci A Public Protein Soc 10(3):668–673

Wang C, Stewart RJ, Kopecek J (1999) Hybrid hydrogels assembled from synthetic polymers and coiled-coil protein domains. Nat Lett 397:417–421

Wong VW, Rustad KC, Galvez MG, Neofytou E, Glotzbach JP, Januszyk M, Major MR, Sorkin M, Longaker MT, Rajadas J, Gurtner GC (2011) Engineered pullalan-collagen composite dermal hydrogels improve early cutaneous wound healing. Tissue Eng 17:631–644

Wood CW, Bruning M, Ibarra AA, Bartlett GJ, Thomson AR, Sessions RB, Brady RL, Woolfson DN (2014) CCBuilder: an interactive web-based tool for building, designing and assessing coiled-coil protein assemblies. Bioinformatics 30(21):3029–3035

Wu K, Yang J, Liu J, Kopeček J (2012) Coiled-coil based drug-free macromolecular therapeutics: in vivo efficacy. J Control Release 157:126–131

Xu C, Kopeček J (2008) Genetically engineered block copolymers: influence of the length and structure of the coiled-coil blocks on hydrogel self-assembly. Pharm Res 25(3):674–682

Xu C, Liu R, Mehta AK, Guerrero-Ferreira RC, Wright ER, Dunin-Horkawicz S, Morris K, Serpell LC, Zuo X, Wall JS, Conticello VP (2013) Rational design of helical nanotubes from self-assembly of coiled-coil lock washers. J Am Chem Soc 135(41):15565–15578

Yao M-H, Yang J, Du M-S, Song J-T, Yu Y, Chen W, Zhao Y-D, Liu Y-D (2014) Polypeptide-engineered physical hydrogels designed from the coiled-coil region of cartilage oligomeric matrix protein for three-dimensional cell culture. J Mat Chem B 2(20):3123

Yonekura K, Maki-Yonekura S, Namba K (2003) Complete atomic model of the bacterial flagellar filament by electron cryomicroscopy. Nature 424(6949):643–650

Yu YB (2002) Coiled-coils: stability, specificity, and drug delivery potential. Adv Drug Deliv Rev 54(8):1113–1129

Zimenkov Y, Dublin SN, Ni R, Tu RS, Breedveld V, Apkarian RP, Conticello VP (2006) Rational design of a reversible pH-responsive switch for peptide self-assembly. J Am Chem Soc 128:6770–6771